



This is a repository copy of *Symmetrical Catalytically Active Colloids Collectively Induce Convective Flow*.

White Rose Research Online URL for this paper:
<http://eprints.whiterose.ac.uk/131131/>

Version: Accepted Version

Article:

Gregory, D.A. orcid.org/0000-0003-2489-5462 and Ebbens, S.J. orcid.org/0000-0002-4727-4426 (2018) Symmetrical Catalytically Active Colloids Collectively Induce Convective Flow. *Langmuir*, 34 (14). pp. 4307-4313. ISSN 0743-7463

<https://doi.org/10.1021/acs.langmuir.8b00310>

Reuse

Items deposited in White Rose Research Online are protected by copyright, with all rights reserved unless indicated otherwise. They may be downloaded and/or printed for private study, or other acts as permitted by national copyright laws. The publisher or other rights holders may allow further reproduction and re-use of the full text version. This is indicated by the licence information on the White Rose Research Online record for the item.

Takedown

If you consider content in White Rose Research Online to be in breach of UK law, please notify us by emailing eprints@whiterose.ac.uk including the URL of the record and the reason for the withdrawal request.



eprints@whiterose.ac.uk
<https://eprints.whiterose.ac.uk/>

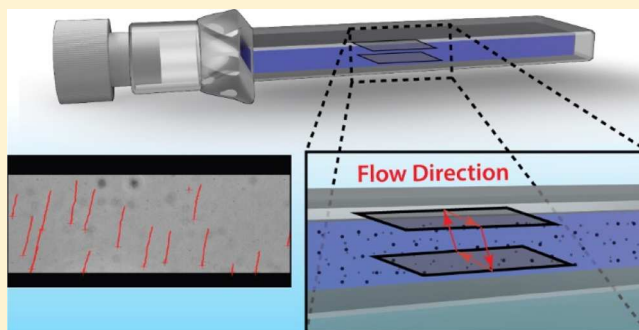
1 Symmetrical Catalytically Active Colloids Collectively Induce 2 Convective Flow

3 David A. Gregory*¹ and Stephen J. Ebbens*²

4 Department of Chemical and Biological Engineering, University of Sheffield, S3 1JD Sheffield, U.K.

5  Supporting Information

6 **ABSTRACT:** Although much attention has focused on self-
7 motile asymmetrical catalytically active “Janus” colloids as a
8 route to enable new fluidic transport applications, the motion
9 of symmetrical catalytically active colloids is less investigated.
10 This is despite isotropically active colloids being more
11 accessible and commonly used as supports for heterogeneous
12 catalysis. Here, we addressed this by systematically investigat-
13 ing the motion of platinum-coated colloids capable of
14 isotropically decomposing hydrogen peroxide. We observed
15 the onset of collective convective flow as the colloidal volume
16 fraction increased above a threshold. The ballistic velocities
17 induced by the collective flow were quantified by particle
18 tracking and were found to increase with the volume fraction. We also determined the associated increase in the Péclet number as
19 an evidence of the potential to use convection as a simple method to enhance mass transport rates. By determining the
20 persistence lengths, we were able to correlate the magnitude of convective flow with the overall catalytic activity per unit volume.
21 This suggests that the mechanism for the collective flow is driven by chemical activity-induced local density differences. Finally,
22 we discussed these results in the context of potential new fluidic applications and highlighted the role that activity-induced
23 convection may play in experiments designed to investigate self-motile catalytic systems.



24 ■ INTRODUCTION

25 Investigating the motion of catalytically active colloids capable
26 of decomposing fuel molecules dissolved in a surrounding
27 fluidic medium has become an area of significant interest over
28 the last decade.¹ A significant amount of research in this area
29 has focused on asymmetrical catalytically active “Janus” colloids
30 that are able to produce enhanced motion by self-phoretic
31 mechanisms or bubble release.^{2–7} The capacity to utilize these
32 catalytically propulsive colloids to enable a wide range of new
33 fluidic applications in disciplines, including medical diagnostics,
34 drug delivery, and environmental remediation, has been a key
35 driver for this effort.⁸ However, much less attention has been
36 given to experimentally determining the motion phenomena for
37 colloids performing catalytic reactions symmetrically over their
38 entire surface. This is somewhat surprising, given the direct
39 relevance to catalytic processes performed using isotropic
40 distributions of the catalyst at a colloidal surface.⁹ Recently, we
41 partially addressed this issue by documenting the chaotic
42 bubble propulsive motion of symmetrical catalytically active
43 colloids.¹⁰ However, bubble propulsion is not typical for
44 uniformly active catalytic colloids, as it requires at least one
45 gaseous reaction product, high surface reactivity,¹¹ and a large
46 enough colloid radius to make the bubble nucleation
47 energetically favorable.¹² Some theoretical studies have
48 investigated the potential for enhanced motion for the more
49 general case of a propulsive symmetrically catalytic active
50 colloid without bubble propulsion. In one example, analysis of

self-generated phoretic mechanisms in isolated individual
51 symmetrical catalytically active colloids suggests that short-
52 time scale deviations from conventional Brownian diffusion will
53 be observed.¹³ Additionally, the ability of individual isotropic
54 catalytically active colloids above a certain size to undergo self-
55 sustained phoretic motion has been theoretically predicted.¹⁴
56 However, there are little existing experimental data to allow
57 these predicted phoretic motion phenomena for isotropic
58 catalytic colloids to be tested. Also, very recently, the possibility
59 for a single symmetrical catalytically active colloid to undergo
60 motion due to the self-generation of convection currents in a
61 solid-walled container has been explored theoretically.¹⁵ This
62 latter phenomena of chemical activity-induced fluid convection
63 is driven by heat evolution and/or the differences in the density
64 of the reactant and product molecules involved in the catalytic
65 reaction.¹⁶ However, it is important to highlight that the
66 phenomenology for convection is fundamentally different from
67 self-phoresis: convection results in the entire bulk fluid moving,
68 whereas self-phoresis causes individual colloids to move
69 through the surrounding fluid, with a rapidly decaying local
70 flow field. A related experimentally demonstrated example of
71 chemical-induced convection, the ability of fixed solid surfaces
72 decorated with areas of catalyst to produce convective flows,⁷³

Received: January 29, 2018

Revised: March 19, 2018

Published: March 21, 2018

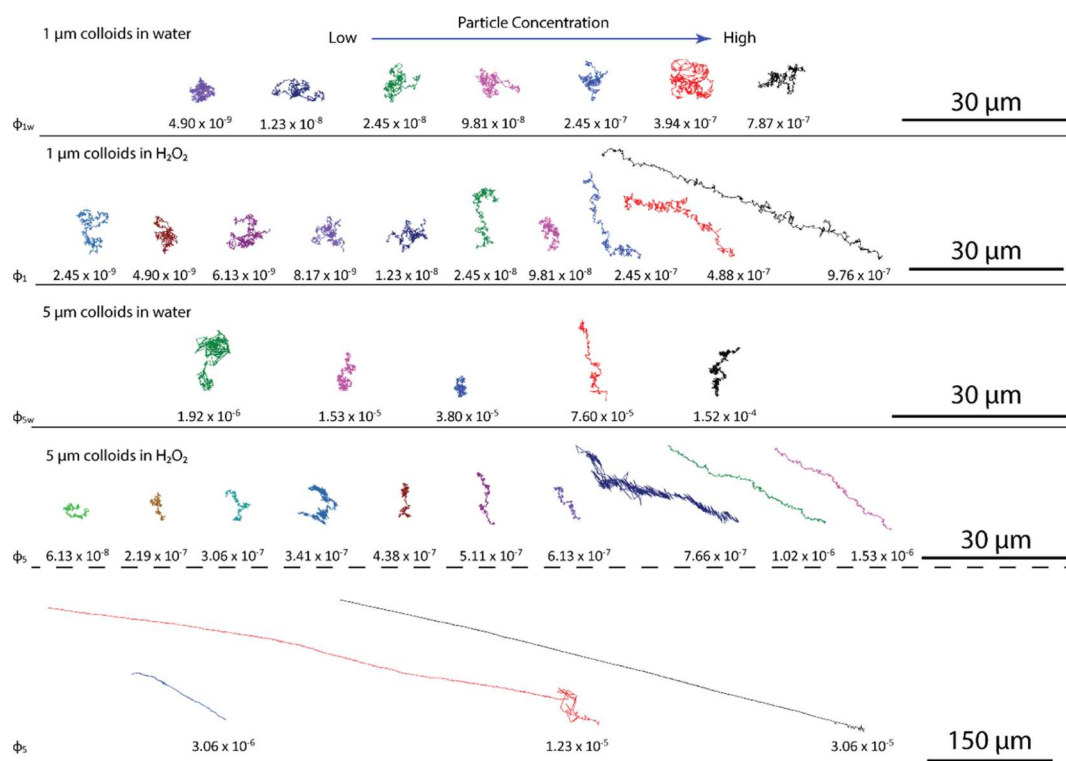


Figure 1. Representative trajectory data (30 s duration) for 1 and 5 μm colloids at varying particle concentrations in water and 10 w/v % hydrogen peroxide. Particle concentrations and equivalent volume fractions are shown below each trajectory.

74 has recently been proposed as a useful method of microfluidic
 75 pumping.^{17,18} Whereas a similar collective fluid flow has been
 76 observed during previous experiments involving catalytic
 77 colloid systems,¹⁹ systematic experiments to isolate and
 78 investigate the onset, character, and origin of this motion are
 79 lacking. This paucity of attention may partly stem from these
 80 drift phenomena being viewed as undesirable, as they hamper
 81 the study of self-phoretic or bubble release motility, which is
 82 the strong current focus of the active colloid research
 83 community. However, convective motion may in fact be
 84 desirable in a range of scenarios, for example, to enhance fluidic
 85 mixing and stirring and to potentially speed up diffusion-limited
 86 catalytic reactions carried out on colloidal supports. In addition,
 87 these phenomena are potentially more accessible as they do not
 88 rely on engineering a Janus structure at the colloid's surface.
 89 Against this background, here we focus on exploring the
 90 motion of homogeneous catalytically active colloids coated with
 91 platinum decomposing dissolved hydrogen peroxide fuel. The
 92 aim of these experiments is to perform a quantitative analysis of
 93 convective, whole fluid drift and also to determine the presence
 94 of any phoretic propulsion effects of symmetrical colloids. The
 95 peroxide/platinum catalytic system is commonly used to power
 96 bubble-propulsive and self-phoretic devices^{20–22} and so allows
 97 our results to directly inform this field. Furthermore, this
 98 catalyst system provides easily accessible rapid decomposition
 99 kinetics under ambient conditions. In addition, similar reactions
 100 have also been shown to cause fixed catalyst patch convective
 101 pumping, and so these prior data can provide mechanistic
 102 insights to aid the interpretation of our findings.¹⁷ A recent
 103 theoretical analysis of convection by symmetrical active colloids
 104 was also based on the peroxide/platinum system.¹⁵ Note that
 105 despite the decomposition of hydrogen peroxide evolving
 106 gaseous oxygen, the investigations could be performed without

the complication of bubble propulsion by selecting appropriate
 colloidal sizes (smaller than our previous work¹⁰) and surface
 catalytic reaction rates.

We performed experiments over a range of well-defined
 volume fractions based on prior qualitative observations that a
 catalytic colloid drift is associated with high catalytic colloid
 concentrations. Low volume fraction experiments in the
 absence of a collective drift most easily allow the presence of
 any phoretic motion effects in our symmetrical catalytically
 active system to be established. Determining a link between the
 volume fraction and fluid flow will be useful not only to
 deliberately instigate these phenomena where desirable for
 future applications but also to determine limits where accurate
 measurements of phoretic propulsion without convection is
 possible. This latter goal is important, given the increasing
 interest in the collective behavior for self-phoretic colloids.^{23,24}
 Our methodology is to use video microscopy combined with
 image analysis to arrive at quantitative trajectory data for a
 statistically significant number of colloids under each
 experimental condition. These trajectory data are then further
 processed to extract parameters that aid interpretation of
 colloidal diffusive, propulsion, and advection rate, including
 mean square displacements (MSD), Péclet number, and
 persistence length.

EXPERIMENTAL SECTION

Monodisperse polystyrene colloids 1 and 5 μm in diameter were
 chemically coated with platinum via in situ reduction of a platinum salt
 (Kisker Biotech custom synthesis). The coating obtained by this
 method consisted of a homogeneous distribution of 2–5 nm radius
 nanoparticles of platinum that were well-adhered to the surface of the
 colloids. To prepare samples for analysis at a range of volume fractions,
 a dilution series was made from a common aqueous stock colloidal
 suspension. To prepare a sample, aliquots were taken from an

140 appropriate diluted solution and added directly into a cuvette. An
 141 additional equivalent volume of 20 w/v % H_2O_2 was added to obtain
 142 an overall H_2O_2 concentration of 10 w/v %. The remaining cuvette
 143 volume was then filled with 10% aqueous hydrogen peroxide. Prior to
 144 measurement, the sample was mixed via inverting the cuvette several
 145 times. For control experiments with 5 μm diameter colloids in water or
 146 at low volume fractions where there was no convective flow, the
 147 colloids would sediment to the bottom of the cuvette within a few
 148 minutes. In order for us to perform colloid measurements in bulk
 149 solution, the cuvette was inverted periodically as required to resuspend
 150 the colloids to allow free solution observations. Because of our
 151 observations being made in the horizontal observation plane, any
 152 vertical sedimentation velocity possessed by the colloids did not
 153 contribute to the subsequent trajectory analysis. The cuvette used was
 154 a 1 mm quartz cuvette (Hellma no. 110-1-40, path length 1 mm \times 9.5
 155 mm \times 38 mm). Video microscopy of the contents of the cuvette was
 156 performed using an upright optical microscope (Nikon Eclipse
 157 LV100) equipped with an Andor CCD camera (Neo 5.5 sCMOS
 158 5.5 megapixel resolution). To allow the colloidal motion to be
 159 analyzed, videos (frame rate of 33 fps) of at least 1000 frames were
 160 recorded at various positions within the cuvette. The center of mass
 161 for each colloid within the field of view was then determined as a
 162 function of time using custom threshold-based image analysis
 163 algorithms (LabVIEW). MSD and persistence lengths were calculated
 164 from the position/times series data, as described in detail previously.¹⁰
 165 High-magnification video inspection revealed that, in all experiments,
 166 there was no evidence of occurrence of bubble nucleation and
 167 detachment, confirming that the experiments were conducted under
 168 conditions that did not promote motion generation by bubble
 169 propulsion.

170 ■ RESULTS AND DISCUSSION

f1 171 **Figure 1** displays typical 30 s duration trajectories for 1 and 5
 172 μm diameter colloids uniformly coated with platinum in both
 173 water and hydrogen peroxide solutions at increasing volume
 174 fractions. For all conditions, the 1 μm colloids were observed in
 175 the bulk solution near the top or bottom of the cuvette, keeping
 176 a distance of approximately 100 μm away from the walls (to
 177 avoid diffusion hindrance due to the walls). It is clear that the
 178 trajectories of the colloids recorded in water appear similar at
 179 all volume fractions and qualitatively resemble Brownian
 180 diffusion. However, in the presence of hydrogen peroxide, at
 181 higher volume fractions, a directional drift in the trajectories for
 182 both 1 and 5 μm colloids was observed. The extent of the drift
 183 clearly increased with the colloid volume fraction. Strikingly, at
 184 the highest volume fraction observed for the 5 μm colloid, the
 185 drift entirely dominates stochastic motion, and colloids cover
 186 hundreds of microns during the period of observation. To
 187 assess the collective features of this drift phenomena, **Figure 2B**
 188 shows the trajectories of many neighboring 1 μm platinum-
 189 coated colloids in a high-volume fraction sample, for regions
 190 near the upper and lower walls of the cuvette (indicated by the
 191 image planes in **Figure 2A**), recorded consecutively within a
 192 time frame of 1–2 min. These observations allow the individual
 193 trajectories shown in **Figure 1** to be understood in the context
 194 of the collective motion of colloids over a large region of the
 195 cuvette. It is consequently clear that there was an overall
 196 collective movement within each region, evidenced by the drift
 197 of a similar magnitude and direction for each individual colloid.
 198 In addition, it is clear that the collective direction of motion was
 199 reversed between the top and bottom of the cuvette.
 200 Observations at the vertical walls of the cuvette confirmed
 201 that the colloids were sinking and rising in directions consistent
 202 with a continuous cyclical motion illustrated in the inset in
 203 **Figure 2A**. In addition, observations in the middle of the cell
 204 revealed that colloids were mostly undergoing Brownian

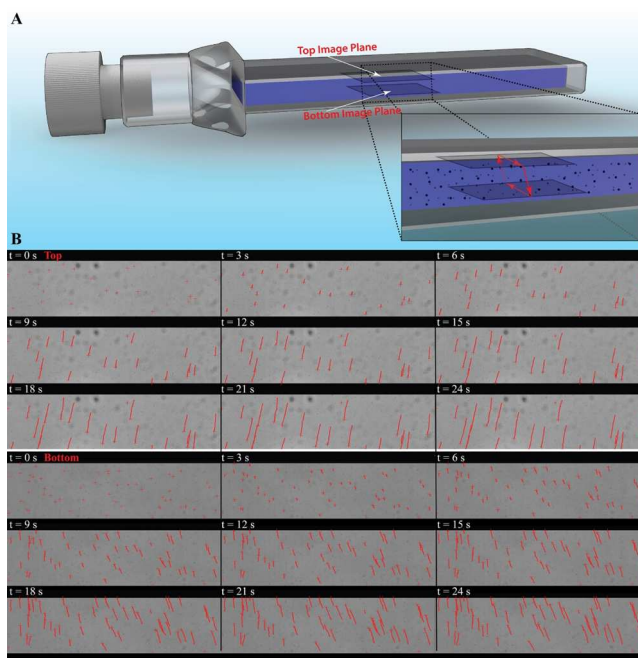


Figure 2. (A) Schematic of the cuvette used in all motion studies. The inset shows the image planes at which the image series were captured, and the red arrows indicate the direction of particle circulation within the cell, determined using video microscopy. (B) Representative time-stamped image sequences recorded at the top and bottom image planes for 1 μm platinum-coated colloids in 10 w/v % H_2O_2 (crosshairs indicate the current position of each colloid in each frame, and red lines show the past trajectory). See also [Video S1](#).

205 motion, without any notable flow affecting the particles (see
 206 [Video S1](#)). Similar circulations were also observed for high
 207 volume fraction samples of 5 μm colloids. This observation that
 208 each colloid moves in a similar direction within a given region
 209 of the cell and the overall continuity of motion within the
 210 cuvette strongly suggest that at high volume fractions, the entire
 211 fluid undergoes a convective flow driven by the catalytic
 212 decomposition of hydrogen peroxide. We note that the
 213 orientation of the circulations of the colloids relative to the
 214 cuvette geometry would vary between different experiments,
 215 indicating that the onset of the collective motion phenomena
 216 may be to some extent chaotic. To illustrate that the entire fluid
 217 was moving, 1 μm fluorescent tracer particles were mixed with
 218 5 μm platinum-coated colloids in water and hydrogen peroxide,
 219 as shown in [Videos S2](#) and [S3](#), respectively.

220 Having understood the qualitative features of our observa-
 221 tions, we now examined the quantitative details that could be
 222 extracted from the colloidal trajectories. To do so, we fitted
 223 MSD curves (ΔL^2) (averaged over observations made for many
 224 colloids at each condition) as a function of the time step (Δt)
 225 to the expression $\Delta L^2 = 4D\Delta t + v^2\Delta t^2$, allowing both the
 226 magnitude of any ballistic velocity, v , and the Brownian
 227 diffusion coefficient, D , to be determined.⁵ To start with, we
 228 considered trajectories recorded at low volume fractions, where
 229 there is no evidence of the collective convection phenomena.
 230 The MSD versus time data in the absence of convection for
 231 both 1 and 5 μm with or without the presence of hydrogen
 232 peroxide fuel colloids was linear (see [Figure S1/S2](#)), consistent
 233 with Brownian diffusion. Furthermore, at low volume fractions,
 234 there was no consistent difference in the diffusion coefficient
 235 attributable to the decomposition of peroxide fuel compared to

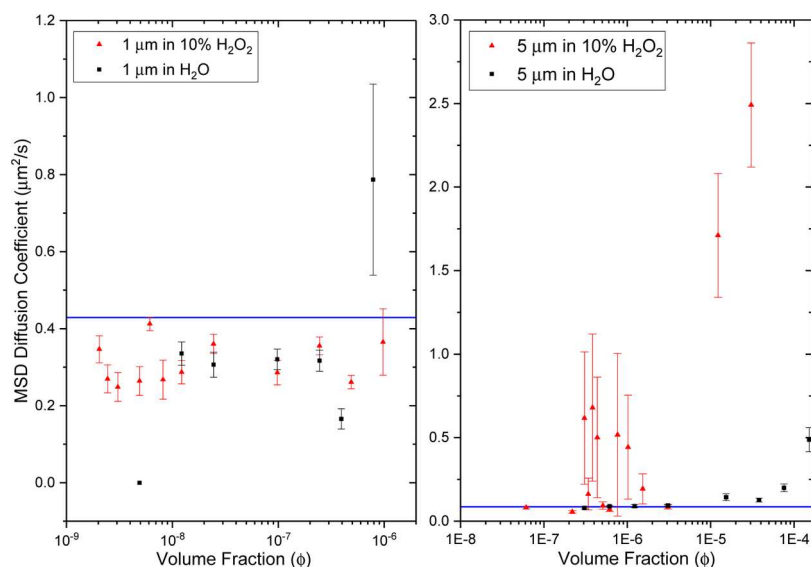


Figure 3. Average diffusion coefficient for 1 and 5 μm uniformly platinum-coated colloids in water and 10% H_2O_2 determined using MSD fitting to the trajectory data. The blue lines indicate the theoretical diffusion coefficients for particles of this size, being $0.429 \mu\text{m}^2/\text{s}$ for 1 μm and $0.086 \mu\text{m}^2/\text{s}$ for 5 μm colloids.

the values measured for catalytically inactive colloids in water (Figure 3). The values of D determined by MSD fitting also showed good agreement with the values calculated using the Stokes–Einstein equation. These data consequently does not provide any evidence that the symmetrical catalytic colloids studied here individually display enhanced or modified motion phenomena such as self-phoresis, subject to the time resolution limits available in this experiment. This finding simplifies the interpretation of the subsequent collective motion phenomena and provides a further justification for using symmetrically active colloids to investigate convection, rather than self-motile Janus colloids.

At the higher volume fractions in the presence of hydrogen peroxide, that is, under the conditions observed to produce a collective drift in the trajectories shown in Figure 1, corresponding MSD curves are parabolic, consistent with colloids that undergo ballistic motion (see Figure S2). Figure 4 displays the ballistic velocities determined by fitting the MSD data as a function of the volume fraction for both catalytically active and inactive colloids (in water). This analysis reveals that at the highest volume fractions, the average velocity was $12 \mu\text{m}$

s^{-1} for active 5 μm colloids and $1.6 \mu\text{m s}^{-1}$ for active 1 μm colloids. For the larger particle size, this velocity is significant and of an equivalent magnitude to that produced by self-phoretic Janus motors, suggesting that useful catalytic transport and pumping effects can be accessed at higher volume fractions even for colloids that are not capable of individually generating enhanced motion by phoresis or bubble propulsion.⁵ It is also clear that significant ballistic velocities are only introduced above a certain volume fraction and that the velocities continue to increase with the volume fraction over the experimental conditions we accessed. In addition, it can be seen that the onset of significant ballistic motion for the 1 μm colloids occurs at a lower volume fraction than for the 5 μm colloids.

Control data for the same colloids measured in water reveal a very slight increase in the ballistic velocity with increasing volume fraction, but all velocities remained less than $0.5 \mu\text{m s}^{-1}$. Although in theory, purely diffusive colloids should give a ballistic velocity of zero, in many previous studies by ourselves and others, a similar nonzero ballistic velocity has been reported for inactive colloids.⁵ This reflects the difficulties in experimentally establishing true Brownian conditions and is the justification for recording these control data, to provide a baseline from which convection or propulsion can be separated. It is likely that thermally induced flow due to microscope illumination may be one factor contributing to this nonzero velocity. As for the increase in this nonzero velocity with the volume fraction, there is no obvious physical mechanism that would account for this, and the trend is in any case somewhat weak. Figure 3 also shows an apparent increase in the diffusion coefficient corresponding to conditions producing appreciable ballistic propulsion, which is likely to be due to cross-talk in the numerical fits, rather than a physical phenomenon. Although our assignment of the nonzero ballistic velocities here to convection is supported by observations of the collective fluid motion within the whole cuvette, we also consider the extent to which MSD analysis alone can be used to distinguish self-propulsion from convection. This is relevant in scenarios where it is difficult or impossible to assess overall colloidal/fluid motion. For the smaller particle size, the MSD curves alone can

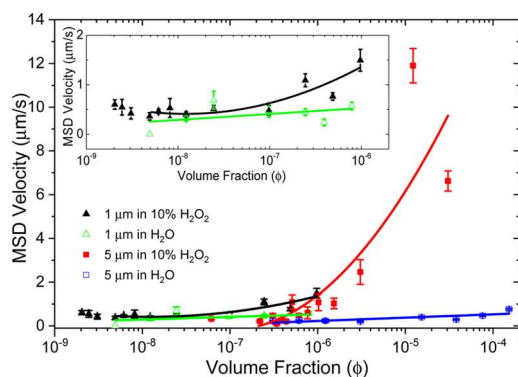


Figure 4. Mean platinum-coated colloid velocity (determined from a quadratic fit to MSD data) for 1 and 5 μm colloids in water and 10 w/v % H_2O_2 as a function of the volume fraction (inset is an expansion for the 1 μm data). Fitted lines are shown to guide the eye.

296 clearly distinguish the behavior we observe here from the case
 297 of an equivalently sized colloid producing a self-propulsion
 298 vector that corotates with the colloid body, such as a self-
 299 phoretic Janus colloid (see Figures S1 and S2). It is well-
 300 established analytically and experimentally that in this case,
 301 rapid Brownian rotation rate (Brownian diffusion time $1\ \mu\text{m}$
 302 colloids $\tau_R^{-1} = 0.78\ \text{s}^{-1}$) means that pure parabolic MSD versus
 303 time step curves are only expected at very short time scales ($\Delta\tau$
 304 $< 1\ \text{s}$) and that beyond this, the MSD will become linear, with a
 305 gradient increase reflecting the degree of enhanced diffusion.²⁵
 306 In this respect, the MSD curves for $1\ \mu\text{m}$ colloids at higher
 307 volume fractions are parabolic MSD over the entire accessible
 308 time scale (30 s) and so not consistent with corotating self-
 309 propulsion (see Figures S3 and S4). Instead, convective drift, in
 310 the regions of the cuvette we performed analysis in, is well-
 311 approximated by Brownian colloids subject to a ballistic
 312 propulsion vector with a constant velocity and magnitude.
 313 However, for the $5\ \mu\text{m}$ colloids, the Brownian rotation rate is
 314 much slower (Brownian diffusion time $5\ \mu\text{m}$ colloids $\tau_R^{-1} = 97$
 315 s^{-1}), and the MSD for convection with constant direction or
 316 self-generated corotating propulsion is consequently hard to
 317 distinguish without observing the colloid for a long period. We
 318 also highlight that in this experiment, we analyzed colloidal
 319 motion far from the edges of the cuvette. However, to ensure
 320 fluid continuity, the convective flows' direction does in fact
 321 change in different positions within the cuvette (see Figure 2),
 322 so we can expect complicated MSD curves to be observed near
 323 the boundaries of cuvettes or for fluids constrained in
 324 containers with a complex geometry. In these cases, the
 325 convective propulsion vectors' direction and magnitude in the
 326 plane of analysis will vary.
 327 As a high volume fraction catalytic convection might be
 328 exploited for mass transport applications, it is also useful to
 329 evaluate a Péclet number for our experiments, reflecting the
 330 ratio of advection to the natural Brownian colloidal diffusion
 331 rate. In analogy to a similar analysis for self-phoretic colloids,²⁶
 332 we define the relevant Péclet number, $Pe = vd/D$, where v is the
 333 ballistic velocity, d is the particle diameter, and D is the Stoke-
 334 Einstein calculated diffusion coefficient for the colloid. Figure 5
 335 displays Péclet numbers as a function of the volume fraction
 336 and highlights the order of magnitude increase in this measure
 337 of mass transport that can be achieved for $5\ \mu\text{m}$ catalytically
 338 active colloids simply by increasing their volume fraction.

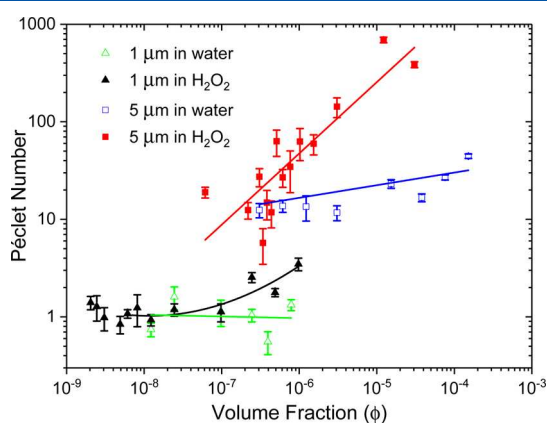


Figure 5. Péclet number for 1 and $5\ \mu\text{m}$ platinum-coated colloids in water and 10% H_2O_2 as a function of the volume fraction. Lines are shown to guide the eye.

Finally, to verify the mechanism for the observed catalytically
 induced convection, we have attempted to normalize the data
 sets obtained for the two differently sized colloids based on the
 overall amount of catalytic activity in each experimental
 condition. This normalization is based on previous theoretical
 and experimental analysis for pumps driven by fixed surface
 bound patches of enzymes, which found that the origin of fluid
 flow is primarily due to the density differences between the
 reagents and the products resulting in convection.¹⁷ Con-
 sequently, the increased overall hydrogen peroxide decom-
 position rate is expected to correlate with an increased degree
 of convection: a link that has been verified for the surface-
 localized enzymatic pumps.¹⁷ In our system, we have previously
 quantified surface reaction rates for the platinum-coated
 colloids: expressed as molecules of hydrogen peroxide
 decomposed per unit surface area, $k_{1\mu\text{m}} = 3.7 \times 10^9 \pm 4.2 \times$
 $10^8\ \text{s}^{-1}\ \mu\text{m}^{-2}$ and $k_{5\mu\text{m}} = 9.6 \times 10^9 \pm 4.2 \times 10^8\ \text{s}^{-1}\ \mu\text{m}^{-2}$, that is,
 the platinum coating of the $5\ \mu\text{m}$ colloid is almost 3 times more
 intrinsically reactive than the coating on the smaller $1\ \mu\text{m}$
 colloids. Note that this difference in reactivity is likely to be due
 to differences in the uncontrolled properties of the different-
 sized chemically coated colloids (e.g., roughness and coating
 thickness), rather than a general finding. These parameters
 allowed us to estimate the overall decomposition rate per mL of
 solution in our experiments. For this analysis, we chose to use
 persistence lengths as our measure of convection, reflecting the
 average length over which a given colloid moves in a constant
 direction, and were thus expected to provide a good indicator
 of the degree of convection for the regions of the cuvette in
 which we performed the analysis. Figure 6 reveals a plot of

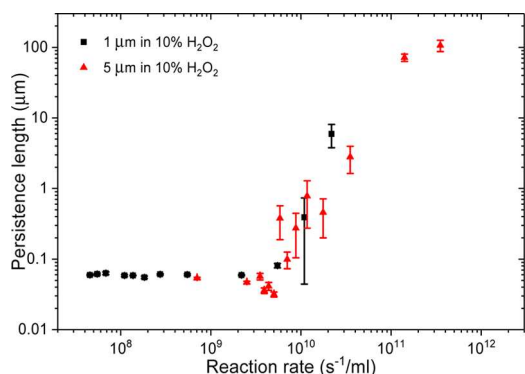


Figure 6. Persistence length as a function of the overall colloid reaction rate per unit volume.

persistence length¹⁰ against the overall colloidal activity per mL
 in the cuvette. The overall catalytic activity was determined by
 evaluating the product of the number density of colloids per
 unit volume, surface area of an individual colloid, and the
 reaction rate per unit area (i.e., reaction rate per unit volume =
 $6\phi k/d$, where d is the diameter of the colloid). This procedure
 produces a good collapse of the data and suggests that a
 criterion of a reaction rate in excess of $5 \times 10^9\ \text{s}^{-1}\ \text{mL}^{-1}$ is
 needed to initiate a convective drift via catalytic activity within
 our particular cuvette geometry.

DISCUSSION

The observation that catalytic activity at the surface of colloids
 can induce bulk convective fluid motion is related to the
 previous use of surface-bound catalytic patches to “pump”

fluids.^{17,18} However, in contrast to fixed catalytic patches, the catalytic colloids that induce the fluid pumping in this study are themselves motile, which opens up new possibilities. For example, our results indicate that the onset of catalytic pumping is instigated only after the accumulation of a certain volume fraction of colloids in a given region, which could be exploited to “switch on” convective mixing at a desired stage of a lab-on-a-chip operation. This convective pumping phenomena hence appear attractive for exploitation in combination with other existing and emerging methods for controlling local colloidal densities. Examples include external colloidal manipulations using magnetic fields and the various self-phoretic and bubble propulsive transport phenomena possessed by catalytic colloids, which can spontaneously result in high volume fraction cluster formation.²⁷ In addition to local mixing and fluid transport applications, collective convective motion in colloids used as catalytic supports for heterogeneous catalysis could speed up diffusion-limited reactions. Indeed, this effect may be present, but not necessarily optimized, in existing catalyst systems.

It is likely that the convective flow observed here arises from the chemical activity generated by density differences around each active colloid. The products of hydrogen peroxide decomposition are less dense than the reagents, which is known to generate a rising convective flow above patches of catalase, performing hydrogen peroxide decomposition.¹⁷ Recently, the way in which this phenomena can produce motion for a single symmetrical catalytically active colloid decomposing hydrogen peroxide in a walled container has been theoretically investigated.¹⁵ Modeling this scenario showed how the density differences generated by the catalytic reaction at the colloid surface lead to fluid flows. When the colloid was positioned away from the center of the container, it experienced asymmetrical flows, resulting in motion toward the container walls, and eventually became trapped at the corner of the container. Removing sharp corners from the containers provided a route to achieve a sustained circulating flow in the presence of a second, passive particle. Although these simulations were performed with the colloids localized at a planar interface and only considered a single active particle, they appear to capture the essence of the phenomena we observe. In our experiment, it is the combination of each individual local density-driven flow and boundary conditions imposed by the cuvette that lead to the observed cyclical motion. An additional potential driving force for motion in our system is thermal-induced convection because of local temperature changes associated with the decomposition reaction. However, this has previously been assessed to be a minor effect in the related case of catalase decomposing hydrogen peroxide.¹⁷

A further result from our work is that we did not find any evidence for modified diffusion phenomena for either 1 or 5 μm diameter symmetrical catalytically active colloids at low volume fractions. However, we note that our experiment does not have the temporal resolution to assess the anomalous diffusion phenomena suggested by Golestanian,¹³ and our system may not meet the criteria required for the suggested Autophoretic mechanism.¹⁴ On this basis, verifying self-phoretic phenomena for symmetrical colloids will require further study.

Finally, in addition to the potential to positively exploit the collective convection reported here, convection remains a significant challenge when investigating self-phoresis and other catalytically induced motility phenomena. Here, we have

identified a threshold for the catalytic collective convection onset based on the total colloidal chemical activity per unit fluid volume. Although this onset parameter may be specific to our cuvette geometry, it is likely that the flows we observed are a general phenomenon for experiments where catalytic colloids, symmetrical or otherwise, are confined for observation and perform reactions that can generate density variations. It consequently appears that when conducting experiments beyond a certain volume fraction/catalytic activity level, convective motion will be inevitable. Here, we have also shown that for individual colloids, the resulting trajectories can be hard to distinguish from self-phoretic effects even with the use of MSD analysis. These findings emphasize the requirement for researchers quantifying the motion of catalytic colloids to use methods that can identify convective motion. These include looking for cyclical patterns of collective motion and deploying inactive tracer particles as required to reveal bulk fluid flow.

CONCLUSIONS

We have studied the motion of 1 and 5 μm diameter colloids symmetrically coated with platinum while catalytically decomposing dissolved hydrogen peroxide. At low volume fractions, individual catalytically active colloids' motion was indistinguishable from Brownian diffusion. However, as the volume fraction increased, the onset of collective cyclical convective flow was observed. Particle tracking and MSD trajectory analysis were used to quantify the ballistic propulsion velocity due to the convective flow, which was found to progressively increase with the volume fraction. The magnitude of convective drift, quantified using persistence lengths, was found to be well-correlated with the reaction rate per unit volume of solution for both colloid sizes. On this basis, it is likely that the mechanism driving the flow is the solution density variations produced by the catalytic reaction. The convective flow significantly increases the colloidal Péclet number, suggesting applications for mass transport. Deliberately exploiting this volume fraction-dependent phenomena provides a potential new route to instigate fluid pumping in lab-on-a-chip systems. Additionally, there is potential to control the convective flow to enhance the reaction rate during the diffusion-limited heterogeneous catalysis. We also highlight that collective convective motion is likely to occur in many experiments designed to investigate self-motile catalytic systems, rendering it important that appropriate protocols are used to distinguish convection from self-propulsion. In this respect, we hope this study will be of relevance to other experimentalists working in the area of active colloid research.

ASSOCIATED CONTENT

Supporting Information

The Supporting Information is available free of charge on the ACS Publications website at DOI: 10.1021/acs.langmuir.8b00310.

Partial and full MSD curves for 1 and 5 μm platinum-coated polystyrene colloids in water and 10% v/wt hydrogen peroxide at low and high volume fractions (PDF)

Platinum-coated colloids (1 μm) in 10% v/w hydrogen peroxide undergoing induced convective flow in the cuvette at the top, middle, and bottom image planes over a time frame of 30 seconds (ZIP)

505 Platinum-coated colloids (5 μm) in water with 1 μm
506 fluorescent polystyrene tracer particles undergoing
507 Brownian motion (ZIP)
508 Platinum-coated colloids (5 μm) in 5% v/w hydrogen
509 peroxide with 1 μm fluorescent polystyrene tracer
510 particles undergoing convective flow (ZIP)

511 ■ AUTHOR INFORMATION

512 Corresponding Authors

513 *E-mail: d.a.gregory@sheffield.ac.uk (D.A.G.).

514 *E-mail: s.ebbens@sheffield.ac.uk (S.J.E.).

515 ORCID

516 David A. Gregory: 0000-0003-2489-5462

517 Stephen J. Ebbens: 0000-0002-4727-4426

518 Author Contributions

519 The manuscript was written through contributions of all
520 authors. All authors have given approval to the final version of
521 the manuscript. The authors contributed equally.

522 Funding

523 The authors would like to acknowledge support from the
524 EPSRC, S.J.E. Career Acceleration Fellowship (EP/J002402/1
525 and EP/N033736/1).

526 Notes

527 The authors declare no competing financial interest.

528 ■ ABBREVIATIONS

529 MSD mean squared displacement

530 CCD charge-coupled device

532 ■ REFERENCES

533 (1) Dey, K. K.; Wong, F.; Altemose, A.; Sen, A. Catalytic Motors—
534 Quo Vadimus? *Curr. Opin. Colloid Interface Sci.* **2015**, *21*, 4–13.
535 (2) Brown, A. T.; Poon, W. C. K. How Platinum-Coated Janus
536 Particles Swim. **2013**, *1*, 9.
537 (3) Lee, T. C.; Alarcón-Correa, M.; Miksch, C.; Hahn, K.; Gibbs, J.
538 G.; Fischer, P. Self-Propelling Nanomotors in the Presence of Strong
539 Brownian Forces. *Nano Lett.* **2014**, *14*, 2407–2412.
540 (4) Ke, H.; Ye, S.; Carroll, R. L.; Showalter, K. Motion Analysis of
541 Self-Propelled Pt–silica Particles in Hydrogen Peroxide Solutions. *J.*
542 *Phys. Chem. A* **2010**, *114*, 5462–5467.
543 (5) Howse, J. R.; Jones, R. A. L.; Ryan, A. J.; Gough, T.; Vafabakhsh,
544 R.; Golestanian, R. Self-Motile Colloidal Particles: From Directed
545 Propulsion to Random Walk. *Phys. Rev. Lett.* **2007**, *99*, 048102.
546 (6) Gao, W.; Pei, A.; Dong, R.; Wang, J. Catalytic Iridium-Based
547 Janus Micromotors Powered by Ultralow Levels of Chemical Fuels. *J.*
548 *Am. Chem. Soc.* **2014**, *136*, 2276–2279.
549 (7) Baraban, L.; Makarov, D.; Streubel, R.; Mönch, I.; Grimm, D.;
550 Sanchez, S.; Schmidt, O. G. Catalytic Janus Motors on Microfluidic
551 Chip: Deterministic Motion for Targeted Cargo Delivery. *ACS Nano*
552 **2012**, *6*, 3383–3389.
553 (8) Ebbens, S. J. Active Colloids: Progress and Challenges towards
554 Realising Autonomous Applications. *Curr. Opin. Colloid Interface Sci.*
555 **2016**, *21*, 14–23.
556 (9) Sheldon, R. A.; van Pelt, S. Enzyme Immobilisation in
557 Biocatalysis: Why, What and How. *Chem. Soc. Rev.* **2013**, *42*, 6223–
558 6235.
559 (10) Gregory, D. A.; Campbell, A. I.; Ebbens, S. J. Effect of Catalyst
560 Distribution on Spherical Bubble Swimmer Trajectories. *J. Phys. Chem.*
561 *C* **2015**, *119*, 15339–15348.
562 (11) Wang, S.; Wu, N. Selecting the Swimming Mechanisms of
563 Colloidal Particles: Bubble Propulsion versus Self-Diffusiophoresis.
564 *Langmuir* **2014**, *30*, 3477–3486.

(12) Manjare, M.; Yang, B.; Zhao, Y.-P. Bubble Driven
565 Quasioscillatory Translational Motion of Catalytic Micromotors. *Phys. Rev. Lett.* **2012**, *109*, 128305. 567
(13) Golestanian, R. Anomalous Diffusion of Symmetric and
568 Asymmetric Active Colloids. *Phys. Rev. Lett.* **2009**, *102*, 188305. 569
(14) Michelin, S.; Lauga, E.; Bartolo, D. Spontaneous Autophoretic
570 Motion of Isotropic Particles. *Phys. Fluids* **2013**, *25*, 061701. 571
(15) Shklyaev, O. E.; Shum, H.; Yashin, V. V.; Balazs, A. C. 572
Convective Self-Sustained Motion in Mixtures of Chemically Active
573 and Passive Particles. *Langmuir* **2017**, *33*, 7873–7880. 574
(16) Ortiz-Rivera, I.; Shum, H.; Agrawal, A.; Sen, A.; Balazs, A. C. 575
Convective Flow Reversal in Self-Powered Enzyme Micropumps. *Proc.*
576 *Natl. Acad. Sci. U.S.A.* **2016**, *113*, 2585–2590. 577
(17) Sengupta, S.; Patra, D.; Ortiz-Rivera, I.; Agrawal, A.; Shklyaev,
578 S.; Dey, K. K.; Córdova-Figueroa, U.; Mallouk, T. E.; Sen, A. Self-
579 Powered Enzyme Micropumps. *Nat. Chem.* **2014**, *6*, 415–422. 580
(18) Zhou, C.; Zhang, H.; Li, Z.; Wang, W. Chemistry Pumps: A
581 Review of Chemically Powered Micropumps. *Lab Chip* **2016**, *16*,
582 1797–1811. 583
(19) Dunderdale, G.; Ebbens, S.; Fairclough, P.; Howse, J. 584
Importance of Particle Tracking and Calculating the Mean-Squared
585 Displacement in Distinguishing Nanopropulsion from Other Pro-
586 cesses. *Langmuir* **2012**, *28*, 10997–11006. 587
(20) Brown, A.; Poon, W. Ionic Effects in Self-Propelled Pt-Coated
588 Janus Swimmers. *Soft Matter* **2013**, *10*, 4016–4027. 589
(21) Baraban, L.; Makarov, D.; Streubel, R.; Mönch, I.; Grimm, D.;
590 Sanchez, S.; Schmidt, O. G. Catalytic Janus Motors on Microfluidic
591 Chip: Deterministic Motion for Targeted Cargo Delivery. *ACS Nano*
592 **2012**, *6*, 3383–3389. 593
(22) Das, S.; Garg, A.; Campbell, A. I.; Howse, J.; Sen, A.; Velegol,
594 D.; Golestanian, R.; Ebbens, S. J. Boundaries Can Steer Active Janus
595 Spheres. *Nat. Commun.* **2015**, *6*, 8999. 596
(23) Wang, W.; Duan, W.; Ahmed, S.; Sen, A.; Mallouk, T. E. From
597 One to Many: Dynamic Assembly and Collective Behavior of Self-
598 Propelled Colloidal Motors. *Acc. Chem. Res.* **2015**, *48*, 1938–1946. 599
(24) Zöttl, A.; Stark, H. Emergent Behavior in Active Colloids. *J.*
600 *Phys.: Condens. Matter* **2016**, *28*, 253001. 601
(25) Ebbens, S.; Tu, M.-H.; Howse, J. R.; Golestanian, R. Size
602 Dependence of the Propulsion Velocity for Catalytic Janus-Sphere
603 Swimmers. *Phys. Rev. E: Stat., Nonlinear, Soft Matter Phys.* **2012**, *85*,
604 020401. 605
(26) Sabass, B.; Seifert, U. Dynamics and Efficiency of a Self-
606 Propelled, Diffusiophoretic Swimmer. *J. Chem. Phys.* **2012**, *136*,
607 064508. 608
(27) Theurkauff, I.; Cottin-Bizonne, C.; Palacci, J.; Ybert, C.;
609 Bocquet, L. Dynamic Clustering in Active Colloidal Suspensions with
610 Chemical Signaling. *Phys. Rev. Lett.* **2012**, *108*, 268303. 611